Mikada, H., Moore, G.F., Taira, A., Becker, K., Moore, J.C., and Klaus, A. (Eds.)
Proceedings of the Ocean Drilling Program, Scientific Results Volume 190/196

17. Velocity Analysis of LWD Sonic Data in Turbidites and Hemipelagic Sediments Offshore Japan, ODP Sites 1173 and 808[1]

David Goldberg,[2] Arthur Cheng,[3] Sean Gulick,[4] Joakim Blanch,[3] and JoongMoo Byun[5]

ABSTRACT

Logging-while-drilling (LWD) sonic data collected during Ocean Drilling Program Leg 196 in low-velocity turbidites and hemipelagic sediments were analyzed to extract *P*-wave velocity using high-resolution dispersion analysis and appropriate tool and borehole modeling. The sonic waveform data show an overall increase in velocity with decreasing frequency. Numerical modeling indicates that velocity computations should be made in the frequency band of highest waveform energy. Estimates of velocity using this approach compare well with core data and wireline sonic logs at the reference site (Site 1173), whereas conventional semblance analysis and dispersion corrections using a look-up table tend to underestimate the velocity by as much as 10%. Synthetic seismograms computed using this approach from the LWD sonic data correlate well to seismic reflection profiles at Site 1173. At Site 808, correlation of synthetic seismograms from our LWD data analysis suggests that transverse velocity anisotropy is present in the prism sediments. High-resolution dispersion analysis is recommended for velocity analysis from LWD sonic data in similar low-velocity marine sediments.

[1]Goldberg, D., Cheng, A., Gulick, S.P.S., Blanch, J., and Byun, J., 2005. Velocity analysis of LWD sonic data in turbidites and hemipelagic sediments offshore Japan, ODP Sites 1173 and 808. *In* Mikada, H., Moore, G.F., Taira, A., Becker, K., Moore, J.C., and Klaus, A. (Eds.), *Proc. ODP, Sci. Results,* 190/196, 1–15 [Online]. Available from World Wide Web: <http://www-odp.tamu.edu/publications/190196SR/VOLUME/CHAPTERS/352.PDF>. [Cited YYYY-MM-DD]
[2]Borehole Research Group, Lamont-Doherty Earth Observatory, PO Box 1000, 61 Route 9W, Palisades NY 10964, USA.
goldberg@ldeo.columbia.edu
[3]SensorWise, Inc., 2908 Rodgerdale Road, Houston TX 77042-4119, USA.
[4]Institute for Geophysics, Jackson School of Geosciences, University of Texas, 4412 Spicewood Springs Road, Building 600, Austin TX 78759, USA.
[5]Department of Earth, Atmospheric, and Planetary Sciences, Massachusetts Institute of Technology, E34-366, 77 Massachusetts Avenue, Cambridge MA 02139-4307, USA.

Initial receipt: 3 November 2003
Acceptance: 19 October 2004
Web publication: 7 January 2005
Ms 196SR-352

INTRODUCTION

Sonic velocity logs provide one of the best means to investigate the physical properties and porosity of drilled sequences and to tie logging data with seismic and core measurements. Increasingly, these measurements are required in shallow-marine sediments where *P*-wave velocity is extremely low, often close to the fluid velocity, for geotechnical and shallow seismic exploration. Such low velocity values make the analysis of sonic logs from logging-while-drilling (LWD) measurements difficult because of the strong effects of wave modes linked to the presence of a logging tool in the borehole, such as dipole and leaky-P modes, which typically have high amplitudes and are dispersive (e.g., Paillet and Cheng, 1986).

In this paper, we present results from an LWD sonic tool deployed in shallow turbidites and hemipelagic carbonate muds offshore Japan (Mikada, Becker, Moore, Klaus, et al., 2002). The Schlumberger ISONIC LWD tool was used for the first time in the Ocean Drilling Program (ODP) at two sites during Leg 196, penetrating from the seafloor to 750 meters below seafloor (mbsf) at Site 1173 and from 156 to 1025 mbsf at Site 808. More than 1770 m of LWD sonic waveform data were successfully recorded. Mikada, Becker, Moore, Klaus, et al. (2002) and Yoneshima et al. (2003) describe preliminary attempts to compute compressional velocity (V_P) logs from the trapped leaky-P (Airy) wave mode in these data. We produce new V_P estimates from the LWD sonic waveforms using high-resolution dispersion analysis (Blanch et al., 2003) and compare the results with both core data and wireline logs acquired at Site 1173, which was drilled through a relatively homogeneous section of hemipelagic sediments with generally high core recovery (Moore et al., 2001; **Goldberg,** this volume). We also explain differences between our results and previous estimates using the leaky-P mode by numerical modeling of the LWD tool response in the borehole. This paper refers to the *P*-wave slowness, the inverse of V_P, throughout in typical units of microseconds per foot (µs/ft) for analytical computations.

LWD SONIC WAVEFORM DATA

The LWD sonic tool is 17 cm (6.75 in) in diameter, and the hole was drilled with a 25-cm (9.875 in) bit. The tool records four waveforms over an array of receivers spanning a distance of 3.0–4.2 m from the source at 20-cm intervals (Aron et al., 1997). The tool was configured with a wide-band source function, generating *P*-wave energy over frequencies from ~3 to 13 kHz. Drilling rates were maintained between 35 and 60 m/hr throughout the hole, and waveform data were recorded within ~20 min of bit penetration (Mikada, Becker, Moore, Klaus, et al., 2002). At least two depth points, each consisting of eight stacked waveforms, were measured over every 0.30-m interval. Differential caliper logs measuring the distance from the tool to the borehole wall show that both holes are in gauge for the most part, and the quality of the waveforms is not degraded by borehole conditions at Site 1173 and only affected near the décollement fault at Site 808. The recorded waveforms have relatively high signal amplitude because drilling noise is strongly attenuated in these high-porosity sediments.

Figure **F1** shows the time-domain data and frequency spectra of stacked waveforms from the ISONIC tool at three different depths at

F1. LWD sonic waveforms and frequency spectra, p. 9.

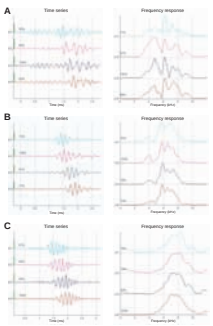

Site 1173. Peak frequency of the waveforms falls between ~6 and 7 kHz. Slowness dispersion plots derived from the four-channel waveforms provide a measure of the energy arriving at a specific slowness over a range of frequency points. Figure F2 shows the computed slowness dispersion using the method outlined by Blanch et al. (2003) for the waveform data at the three depths shown in Figure F1. The maximum of the recorded energy occurs at ~6–7 kHz. Figure F2 clearly illustrates that dispersion is present in the LWD sonic data, showing an overall decrease in slowness with decreasing frequency. Slowness dispersion occurs throughout the hole, but as represented in Figure F2, dispersion is reduced at shallower depths because of the decreasing difference between formation and borehole fluid slowness.

F2. High-resolution slowness dispersion plots, p. 10.

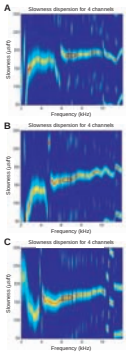

NUMERICAL MODELING

To understand the source of the dispersion observed in these data, we used a finite-difference model to compute waves propagating in a borehole. Waveform modeling provided an opportunity to vary the formation parameters and tool geometries over a wide range and visualize the effects. LWD tool and sediment properties similar to those encountered at Sites 1173 and 808 were considered. We utilized a conventional finite difference method to model a monopole source on a rigid tool in cylindrical geometry (Cheng et al., 1992). This differs significantly from a mode-search computation to track the leaky P-mode dispersion, as used by Yoneshima et al. (2003), in that the relative magnitude of various formation and tool modes can be discretely determined. Formation *P*-wave slowness values over the range of 140–190 µs/ft with no attenuation were modeled. *S*-wave slowness values were held constant at 300 µs/ft so that V_P/V_S ratio decreased for these model results. Fluid and formation density values were 1 and 2 g/cm³, respectively. Tool parameters used for the finite difference model were V_P = 51.31 µs/ft, V_S = 94.66 µs/ft, and density = 7.84 g/cm³ for a 6.75-in-diameter solid steel cylinder. The source and receivers were located on the surface, not at the center, of the tool and a 10-kHz Ricker wavelet source was used. The hole diameter for the model was 8.5 in, although diameters of 9.875 and 11 in were also run without significant differences in the outcome. The model results indicated that because of the presence of the tool in the borehole, and the combination of fluid, borehole size, and source frequency used, the formation *P*-wave energy arrives coincident with the maximum energy peak in the recorded signal. Our primary conclusion from the finite difference modeling is that tool and *P*-wave modes are mixed in the frequency and time domains under these physical conditions.

Figure F3 shows the modeled waveforms and frequency spectra at 14 receiver locations spanning a receiver array and is equivalent to the geometry of the ISONIC tool. The input formation slowness of 160 µs/ft in this example is representative of the model results and illustrates similar waveform amplitude to the field data shown in Figure F2. The simulation shows that the steel drill collar of the LWD tool significantly decreases the slowness of the leaky-P wave at lower frequencies, and the borehole fluid increases the slowness at higher frequencies, similar to the trends observed in the field data shown in Figure F2. The simulation confirms the presence of a dispersive *P*-wave mode with maximum arriving energy occurring at ~6–7 kHz. Figure F3 shows the dispersion computation using the 14-channel model data. Slowness estimation at

F3. Synthetic waveforms and frequency spectra, p. 11.

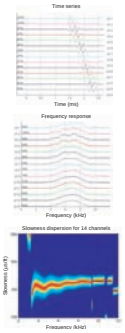

the peak value within the maximum energy band yields the input slowness value of 160 µs/ft. Chosen accurately in this frequency band, the formation slowness estimate does not need additional correction for dispersion effects. The dispersion analysis does not tend toward a low-frequency asymptote equal to the input *P*-wave slowness value as assumed by Yoneshima et al., (2003).

SLOWNESS ANALYSIS

Using high-resolution dispersion analysis (Blanch et al., 2003), we hand-picked a slowness value in the high-energy band to estimate *P*-wave slowness with an accuracy of ±2 µs/ft. Varying the input parameters of this frequency domain computation did not affect the shape of the resulting dispersion curves. We emphasize that at least this amount of uncertainty in the formation slowness estimate still remains using this technique, as dispersion of 1–2 µs/ft can be observed even within our narrow-band analysis window (see Fig. **F2**). As an approximation to the slowness log, we repeated the hand-picking procedure to estimate slowness using the dispersion computation at 3-m (10 ft) depth intervals at Site 1173. Figure **F4** shows these hand-picked points compared to data from laboratory measurements on core samples and to wireline logging data collected during a previous expedition to the site (Moore et al., 2001). The wireline log extends to ~350 mbsf at Site 1173, where the hole closed off below the lithologic boundary between the upper and lower Shikoku Basin facies (Moore et al., 2001). **Goldberg** (this volume) reprocessed slowness values from the wireline logging data. Above 200 mbsf, the wireline and hand-picked estimates are relatively constant and near the upper limit of slowness resolution for both measurements. Below this depth, the wireline slowness values agree closely with the hand-picked estimates, although some localized differences may be expected because of lateral variations in sediment properties between the wireline and LWD holes.

F4. Comparison of slowness values, Site 1173, p. 12.

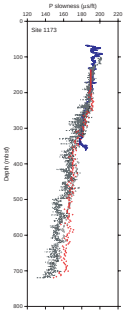

Previous efforts to extract slowness from the ISONIC data at Site 1173 using bandpass filtering and conventional semblance with dispersion corrections using a model-based look-up table are also shown in Figure **F4** (Yoneshima et al., 2003). Overall, the trends of the look-up computation and the hand-picked results show decreasing slowness with depth, characteristic of hemipelagic sediment deposition and compaction over time, and track quite well between 200 and ~490 mbsf. However, the hand-picked estimate and look-up computation trends are consistently separated over this interval with the hand-picked results having 5–10 µs/ft higher slowness values. Below 490 mbsf, as the formation velocity and frequency dispersion increase, the hand-picked and look-up estimates track less well and diverge further with 10–20 µs/ft higher slowness values obtained from the hand-picked estimation.

In addition, we compare these profiles to velocity data measured on core samples at the reference Site 1173, where the lithologic section is relatively undeformed and the core V_P data are largely continuous (Moore et al., 2001). In general, the trends of the core and hand-picked results agree very well between 240 and ~490 mbsf with small ±3-µs/ft variations attributed to one or more of the following effects: (1) lateral changes in properties between the core and LWD holes, (2) sampling bias because of incomplete core recovery, (3) differential porosity rebound of the core samples under ambient laboratory conditions be-

cause of local changes in lithology and cementation, or (4) local fracturing and structures that are not sampled through coring. Because of these effects, comparisons of laboratory and in situ data are often difficult over short intervals and are most useful for overall trend analysis with depth. In general, the trends of both core and hand-picked estimates track well with the previous ISONIC look-up values, indicating normal compaction; however, they both systematically estimate 5–10 µs/ft higher slowness than the look-up results. From ~490–540 mbsf, the core sample and hand-picked estimates are nearly equal, but they diverge below toward lower slowness values and approach the ISONIC look-up results at the bottom of the hole. We suggest that the core data may have preferentially sampled the more compacted (faster) sediments over this lowermost interval. Consistent with this interpretation, the average core recovery dropped dramatically to ~45% below 590 mbsf (Moore et al., 2001). Overall, the hand-picked estimates are more representative of the in situ velocity in this hole.

Similar analysis and comparisons of the LWD sonic results at Site 808 are shown in Figure F5. Overall, slowness varies more as a function of depth at this site. Both the hand-picked and ISONIC look-up results follow similar trends with depth, but the look-up results at this site underestimate the slowness by 10–20 µs/ft. Unlike Site 1173, this difference remains relatively constant over the lowermost 500 m of the hole. Core recovery from previous drilling at Site 808 was poor, and continuous core velocity measurements were too sparse for reliable interpretation of data trends vs. depth at this location, in addition to the difficulties associated with the complicating effects 1–4 noted above.

In the section below, we discuss the implications of the hand-picked ISONIC estimates and compute synthetic seismograms at both Sites 1173 and 808. These computations constrain the integrated velocity profiles computed using the proposed method to known seismic reflections across the study region.

F5. Comparison of slowness values, Site 808, p. 13.

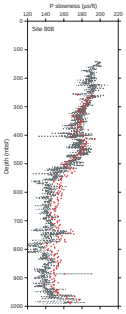

DISCUSSION

Figures F4 and F5 illustrate that the hand-picked slowness values are generally 5–20 µs/ft greater than the ISONIC look-up results, with increasing difference at higher velocities, and correlate better to core measurements within the variation expected over short intervals. Although fast tool modes are accounted for in both of these models and analysis methods, they may still influence the *P*-wave slowness estimate under certain conditions. Analyzed in the time domain with conventional semblance methods (e.g., Kimball and Marzetta, 1984), the presence of the LWD tool broadens the recorded wave arrival, reduces the resolution of the slowness estimate, and obscures the dispersion effects. In this low-velocity environment, subsequently adding a model-based dispersion correction (Brie and Saiki, 1996; Yoneshima et al., 2003) after the slowness is picked reduces the slowness estimate to a value that is not representative of the formation properties and does not match the dispersion curves observed in the LWD sonic data. This is the primary cause of the underestimation of the slowness computed by Yoneshima et al. (2003). The dispersion analysis and hand-picking technique proposed here improves these results substantially; however, it is not a suitable substitute for automatic processing of ISONIC data. In the future, automatic high-resolution dispersion analysis may be adapted for LWD

sonic data without additional dispersion corrections, producing accurate velocity profiles with up to 15-cm vertical sampling at both sites.

Synthetic seismograms were computed using the hand-picked slowness values and the LWD density logs at both sites using Schlumberger GeoQuest software (Figs. F6, F7). Multichannel seismic traces near each site were selected for comparison and are discussed in greater detail by (Moore et al., 2001). At the reference site (Site 1173), LWD data were acquired from seafloor to total depth and a time-depth tie can be accurately made at the seafloor. In Figure F6, the synthetic seismogram correlates well with seismic reflections through the entire reference section and quite closely predicts the transit time to the top of the oceanic crust. The excellent correlation of synthetic and field data at Site 1173 gives confidence that our technique for slowness analysis from ISONIC data is appropriate and the hand-picked estimates of LWD velocity are accurate. We then apply the same computational methods to compare the synthetic and field data in the more complex geological setting at Site 808.

Owing to difficulty in drilling through the deformed prism sediments, the LWD data at Site 808 were recorded only below the casing, and the shallow velocity structure above 156 mbsf is unknown. In Figure F7, depth-time ties are assumed at the depth of the décollement fault (the depth at which LWD operations ceased) and at the seafloor by introducing an arbitrary change in acoustic impedance. Between these two points, the integrated velocity computed from the ISONIC data (1757 m/s) must be increased by 12.5% in order to tie the synthetic with corresponding seismic reflections. The resulting average velocity of 1976 m/s estimated over the sequence from the seafloor to the décollement fault and the synthetic–seismic depth tie at the frontal thrust are both reasonable. We attribute the 12.5% lower integrated LWD velocity at Site 808 to transverse formation anisotropy and fracturing within the accretionary prism, which affect the ISONIC and seismic experiments differently. Assuming that formation anisotropy, fracturing, and faulting are oriented subhorizontally in the prism, the LWD velocity estimates along the axis of the borehole (vertical) will generally be slower than seismic estimates that integrate both vertical and horizontal components. Brueckmann et al. (1993) report transverse velocity anisotropy measurements of up to 15% between the frontal thrust and décollement fault at Site 808. Henry et al. (2003) also provide laboratory evidence of 6%–7% horizontal electrical anisotropy because of strain and shortening in Nankai prism sediment samples. In the presence of such transverse anisotropy at Site 808, a difference between the average velocity estimated from LWD sonic and seismic data can be expected. An in situ estimation of the transverse velocity anisotropy would be required to produce an accurate correlation between the synthetic and field data at this location.

CONCLUSIONS

LWD sonic data were recorded for the first time during ODP Leg 196 at two offshore sites near Japan. Although high signal amplitude was recorded at both sites, the extraction of accurate velocity information in these low-velocity sediments is difficult because the waveforms are dispersive and both leaky-P (Airy) phases and tool modes affect the recorded arrivals. Dispersion of LWD sonic data in low-velocity formations was observed in finite element models, and we attribute this

F6. Synthetic seismogram, Site 1173, p. 14.

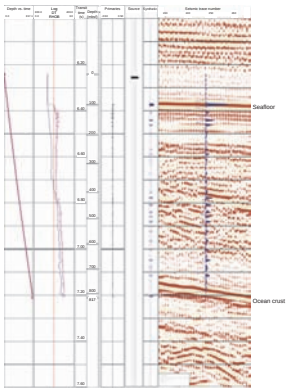

F7. Synthetic seismogram, Site 808, p. 15.

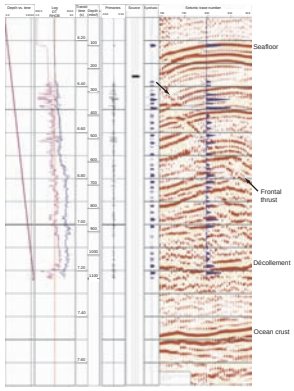

to the presence of the tool in a borehole and not to pure leaky-P mode propagation. *P*-wave slowness was manually estimated from the LWD sonic data at Sites 1173 and 808 using high-resolution dispersion analysis and appropriate frequency band windowing. Estimates of LWD velocity using this approach compare very closely with core and wireline logging results at Site 1173 (reference site) and produce synthetic seismograms that precisely match the basement seismic reflection and constrain the integrated velocity profile. Mismatch between the synthetic and seismic reflection at Site 808 is attributed to the effects of significant velocity anisotropy in the prism sediments. The velocity data described here are available directly via the ODP online logging database at **www.ldeo.columbia.edu/BRG/ODP/DATABASE/index.html.** Conventional analysis methods with additional dispersion corrections using a look-up table tend to underestimate the slowness in these low-velocity marine sediments. In future uses or for automatic processing, high-resolution dispersion analysis in the frequency domain is recommended for LWD sonic data interpretation. In general, LWD tools designed with reduced tool modes may also be necessary to completely discriminate the *P*-wave mode and accurately process the data for formation slowness in similar low-velocity environments.

ACKNOWLEDGMENTS

This research used samples and data provided by the Ocean Drilling Program (ODP). The ODP is sponsored by the U.S. National Science Foundation and participating countries under management of Joint Oceanographic Institutions (JOI), Inc. The NSF/U.S. Science Support Program (USSSP) provided funding for this work. Carl Brenner assisted with preparation of this manuscript. We greatly appreciate the efforts of the crew and staff of the *JOIDES Resolution* during ODP Leg 196 to collect these data and two anonymous reviewers for their suggested improvements to this manuscript. This paper represents LDEO publication number 6589 and UTIG publication number 1663.

REFERENCES

Aron, J., Chang, S.K., Codazzi, D., Dworak, R., Hsu, K., Lau, T., Minerbo, G., and Yogeswaren, E., 1997. Real-time sonic logging while drilling in hard and soft rocks. *Trans. SPWLA Annu. Logging Symp.,* 38:1HH–14HH.

Blanch, J., Cheng, A., Varsamis, G., and Araya, K., 2003. Evaluation of dispersion estimation methods for borehole acoustic data. *SEG Annu. Meet. Expanded Tech. Program Abstr. Biographies,* 77:305–308.

Brie, A., and Saiki, Y., 1996. Practical dipole sonic dispersion correction. *SEG Annu. Meet. Expanded Tech. Program Abstr. Biographies,* 66:178–181.

Brueckmann, W., Moran, K., and Taylor, E., 1993. Accoustic anisotropy and microfabric development in accreted sediment from the Nankai Trough. *In* Hill, I.A., Taira, A., Firth, J.V., et al., *Proc. ODP, Sci. Results,* 131: College Station, TX (Ocean Drilling Program), 221–233.

Cheng, N.Y., Cheng, C.H., and Toksoz, M.N., 1992. Fourth-order finite-difference acoustic logs in transversely isotropic formation. *SEG Annu. Meet. Expanded Tech. Program Abstr. Biographies,* 62:1311–1314.

Henry, P., Jouniaux, L., Screaton, E.J., Hunze, S., and Saffer, D.M., 2003. Anistropy of electrical conductivity record of initial strain at the toe of the Nankai accretionary wedge. *J. Geophys. Res.,* 108:10.1029/2002JB002287.

Kimball, C.V., and Marzetta, T.L., 1984. Semblance processing of borehole acoustic array data. *Geophysics,* 49:274–281.

Mikada, H., Becker, K., Moore, J.C., Klaus, A., et al., 2002. *Proc. ODP, Init. Repts.,* 196 [CD-ROM]. Available from: Ocean Drilling Program, Texas A&M University, College Station TX 77845-9547, USA.

Moore, G.F., Taira, A., Klaus, A., Becker, L., Boeckel, B., Cragg, B.A., Dean, A., Fergusson, C.L., Henry, P., Hirano, S., Hisamitsu, T., Hunze, S., Kastner, M., Maltman, A.J., Morgan, J.K., Murakami, Y., Saffer, D.M., Sánchez-Gómez, M., Screaton, E.J., Smith, D.C., Spivack, A.J., Steurer, J., Tobin, H.J., Ujiie, K., Underwood, M.B., and Wilson, M., 2001. New insights into deformation and fluid flow processes in the Nankai Trough accretionary prism: results of Ocean Drilling Program Leg 190. *Geochem. Geophys. Geosyst.,* 2:10.129/2001GC000166.

Paillet, F.L., and Cheng, C.H., 1986. A numerical investigation of head wave and leaky modes in fluid-filled boreholes. *Geophysics,* 51:1438–1449.

Yoneshima, S., Endo, T., Pistre, V., Thompson, J., Campanac, J., Mikada, H., Moore, J.C., Ienaga, M., Saito, S., and Leg 196 scientific party, 2003. Processing leaky-compressional mode from LWD sonic data in shallow ocean sediments: ODP sites in Nankai Trough. *Proc. 6th SEGJ Int. Symp. Imaging Technology:* Tokyo (SEGJ), 6:45–52.

Figure F1. LWD sonic waveforms and frequency spectra acquired at three source depths in low-velocity marine sediments at Site 1173, offshore Japan. The ISONIC tool recorded four waveforms over a broad frequency band at each source depth. Source depths are (**A**) 167.6, (**B**) 381.0, and (**C**) 685.9 mbsf.

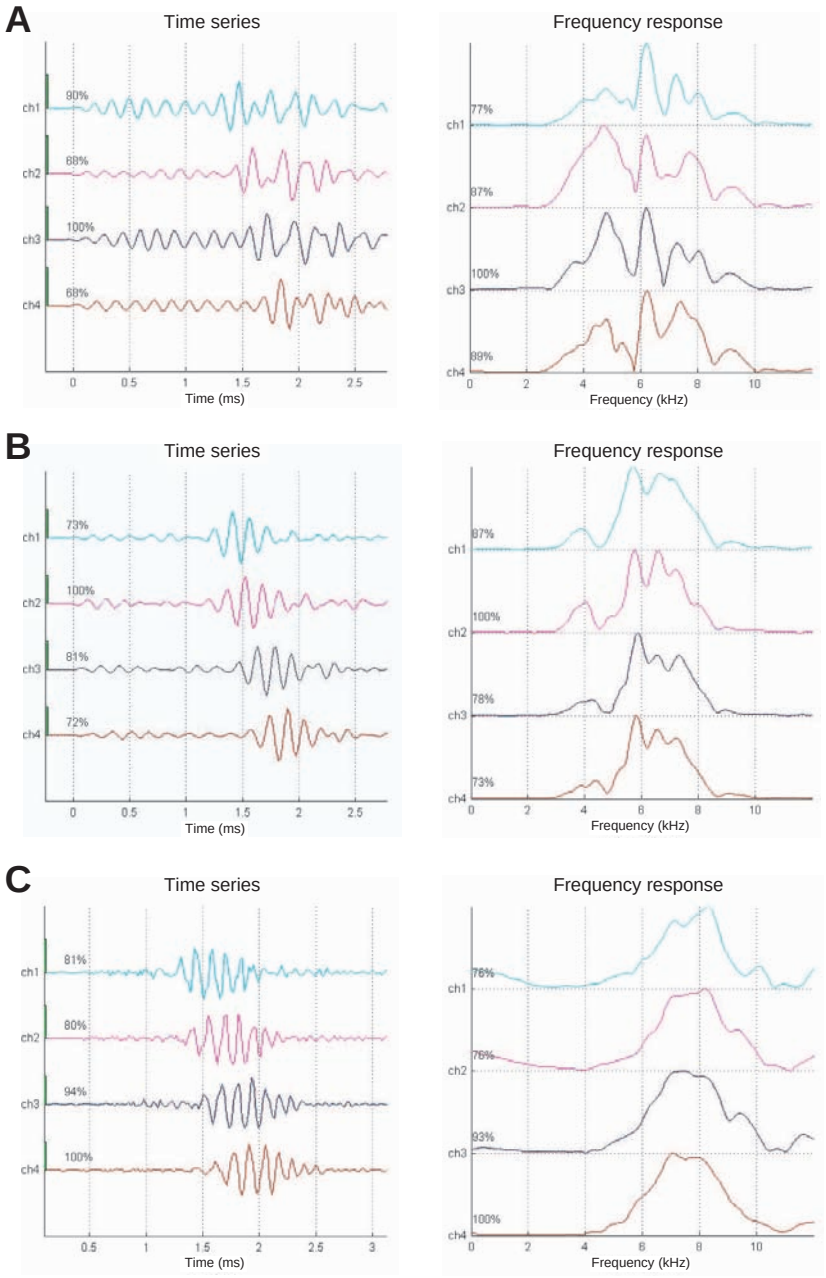

Figure F2. High-resolution slowness dispersion plots of four-channel ISONIC data from Figure F1, p. 9. Color scale corresponds to the semblance value. Dispersion is illustrated by the increase in slowness with frequency. The box indicates the hand-picked frequency band at peak *P*-wave energy levels. Source depths are (**A**) 167.6, (**B**) 381.0, and (**C**) 685.9 mbsf.

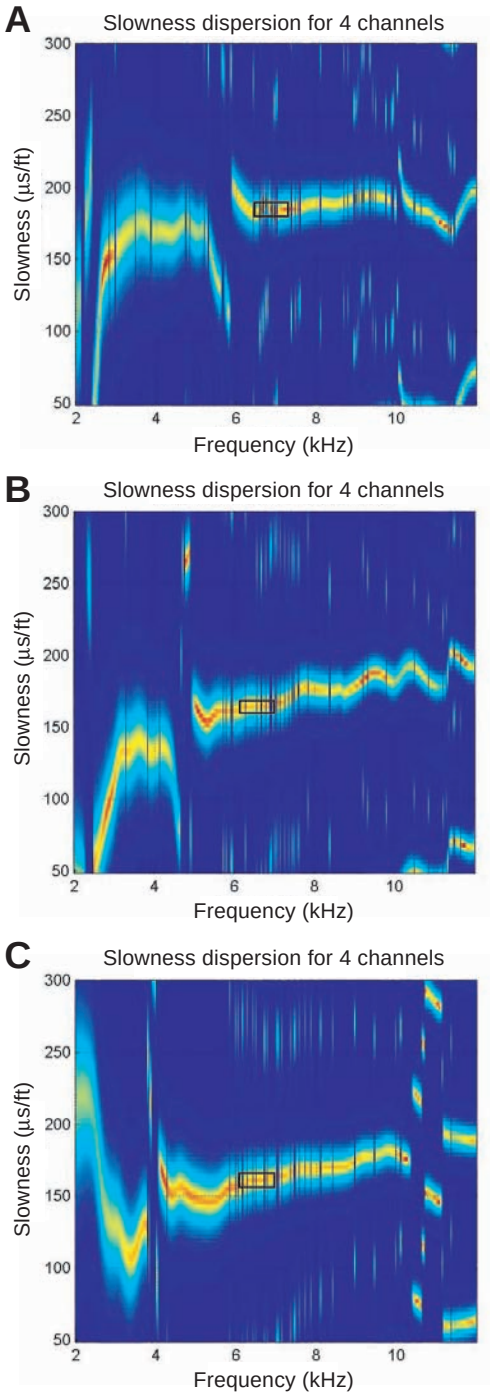

Figure F3. Fourteen synthetic waveforms and frequency spectra using a numerical finite-difference model over an array similar to the ISONIC tool. The input *P*-wave slowness is 160 µs/ft. The observed energy near the 12-kHz of ~150 µs/ft is an artifact of the dispersion analysis. The *P*-wave mode is dispersive over this frequency band.

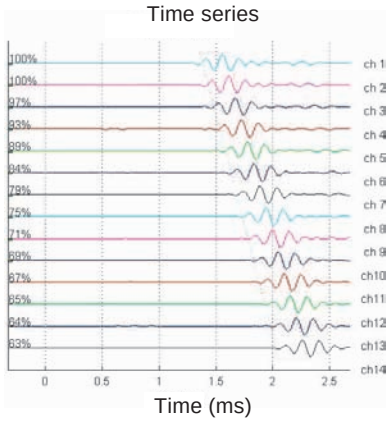

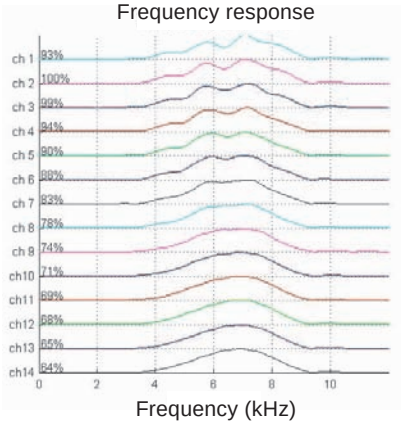

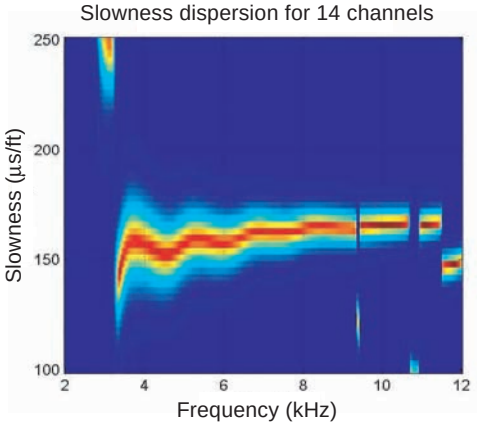

Figure F4. Comparison of slowness values at Site 1173: hand-picked from dispersion plots (red), laboratory core samples (black), conventional semblance with look-up table dispersion corrections (gray), and a wireline sonic log (blue). Hand-picked values generally agree with the core and wireline logging results. Conventional semblance results underestimate slowness by up to 10%, increasing with depth.

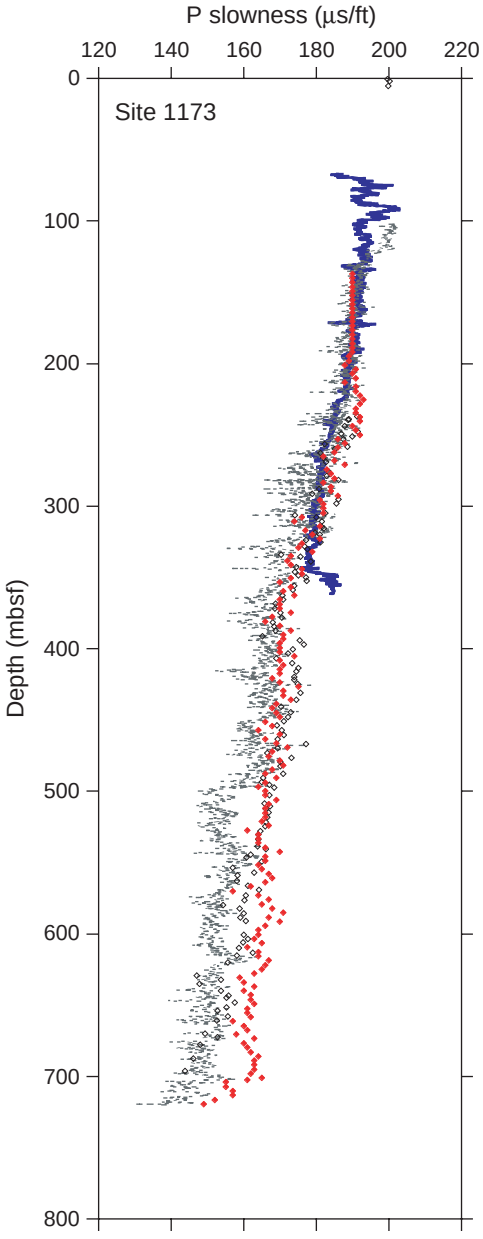

Figure F5. Comparison of slowness values at Site 808: hand-picked from dispersion plots (red) and from conventional semblance with look-up table dispersion correction (gray). Core recovery from previous drilling was poor so that continuous core velocity measurements and data trends vs. depth could not be reliably interpreted at this location. Conventional semblance results underestimate slowness by up to 10% and remain relative constant below 500 mbsf.

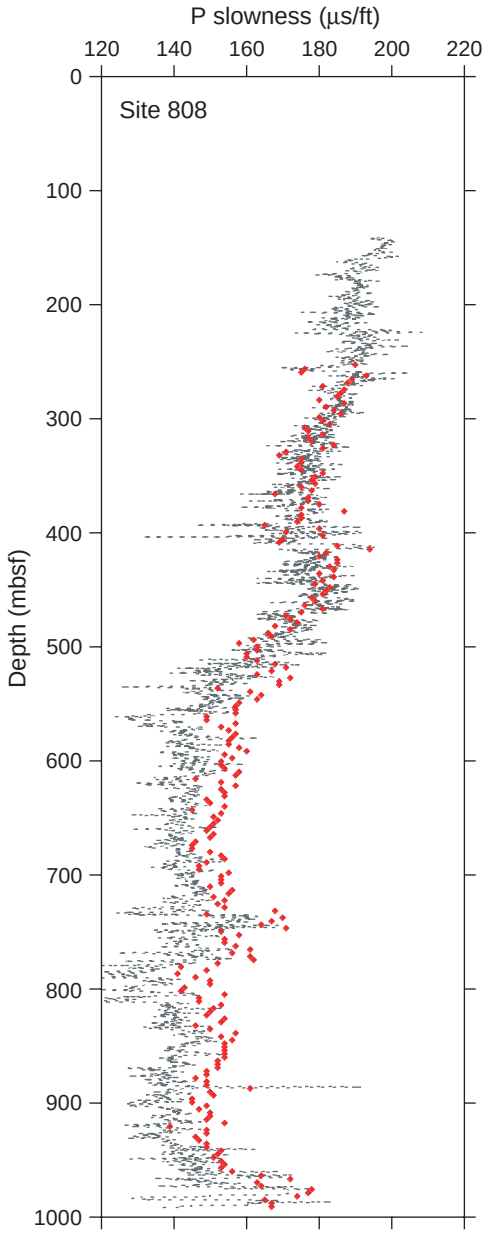

Figure F6. Synthetic seismogram computed from the LWD density log and velocity values hand-picked from ISONIC dispersion plots with field seismic data near the reference site (ODP Site 1173). The LWD data were recorded from seafloor to the total drilled depth of the hole. Integrated transit time and LWD logging curves, the primary reflectors and seismic source, and computed synthetic traces are presented in addition to the synthetic–seismic overlay. The synthetic and seismic reflections at the seafloor and at the top of basement correlate well. RHOB = LWD density (g/cm^3), DT = LWD compressional slowness (ms/ft).

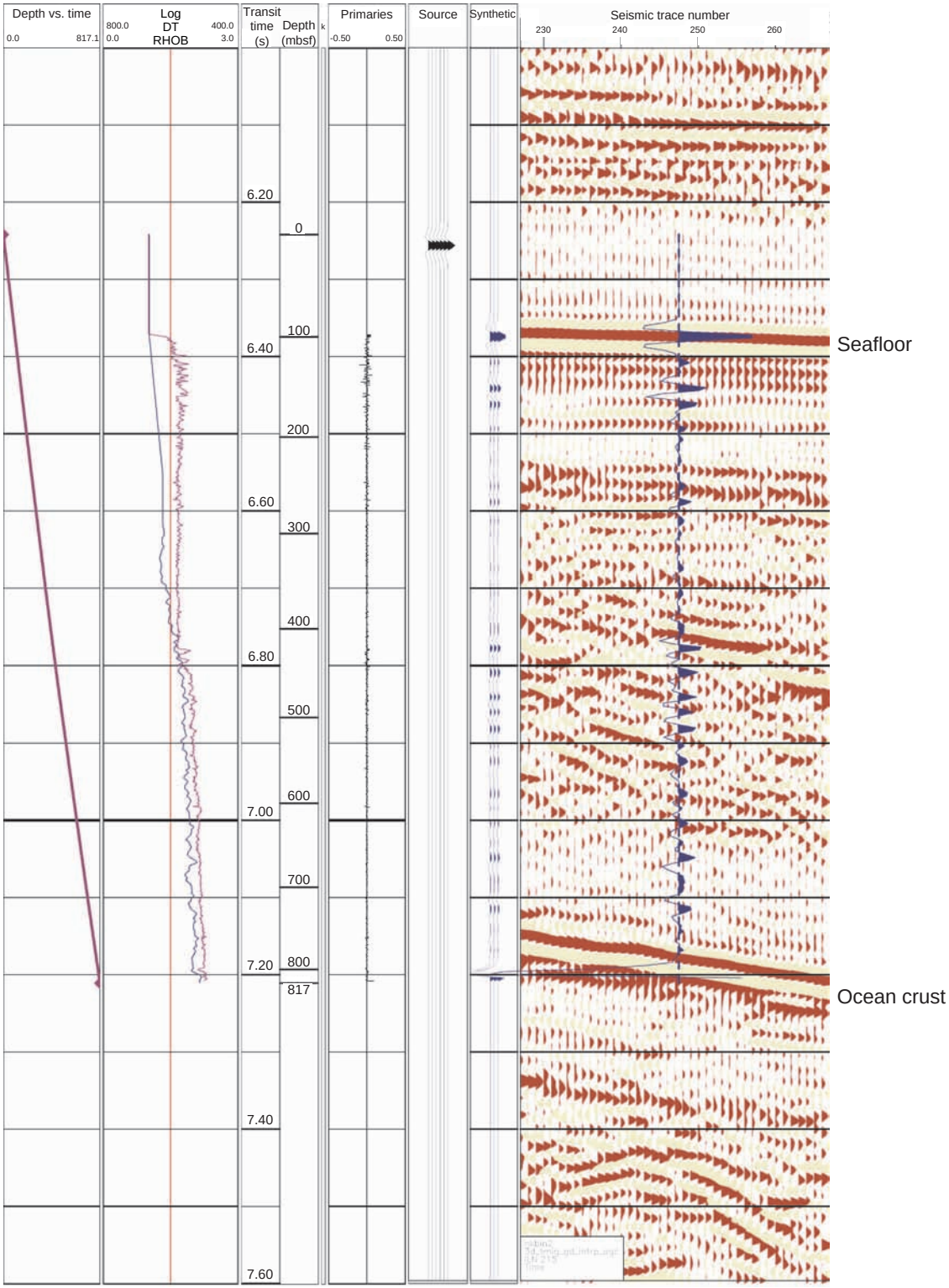

Figure F7. Synthetic seismogram computed from the LWD density log and velocity values hand-picked from ISONIC dispersion plots with field seismic data near the prism site (ODP Site 808). The LWD data were recorded from 160 mbsf to the total drilled depth of the hole, and the shallow velocity structure at this site is unknown. Integrated transit time and LWD log curves, the primary reflectors and seismic source, and computed synthetic traces are presented in addition to the synthetic–seismic overlay. The synthetic and seismic reflections at the seafloor, frontal thrust, and at the décollement fault correlate well after correcting the average LWD velocity for the effect of transverse anisotropy in the prism sediments. RHOB = LWD density (g/cm^3), DT = LWD compressional slowness (ms/ft).